Nuclear Materials and Energy 31 (2022) 101182

Contents lists available at ScienceDirect

Nuclear Materials and Energy

journal homepage: www.elsevier.com/locate/nme

# Research on the normal emissivity of graphite between 150 and 500 °C by an infrared camera for nuclear fusion devices

Shuangbao Shu, Tianqi Wu, Ziyi Wang, Yuzhong Zhang *, Ziqiang Yang, Huajun Liang

*Anhui Province Key Laboratory of Measuring Theory and Precision Instrument, School of Instrument Science and Opto-electronics Engineering, Hefei University of Technology, Hefei 230009, China*

ARTICLE INFO

*Keywords:*
Nuclear fusion device
Graphite
Emissivity
Temperature measurement
Infrared thermography

ABSTRACT

Due to the advantages of high-temperature resistance, low thermal expansion coefficient, and thermal shock resistance, etc., graphite is regarded as one of the materials for the first wall of nuclear fusion devices. The real-time monitoring of temperature distribution of the first wall based on an infrared camera is widely used to guarantee the stable operation of devices. To accurately measure the temperature of the first wall, it is important to measure the normal emissivity of graphite. However, the emissivity of graphite is affected by many factors. For example, the effect of the surface layers, like carbon-hydro layers-layers, will influence the measurement of the emissivity. The ambition of this work is to study the relationship between graphite emissivity and infrared camera with filters of different wavelengths and the roughness of graphite, and then give the proposed emissivity model to improve the accuracy of graphite surface temperature measurement. The experiment is carried out with a FLIR infrared camera and calibrated by using a blackbody furnace. The emissivity at given temperatures is systematically investigated. By using an infrared camera with no filter (band wavelength range of 7.5–13 μm), a $10.2 \pm 0.1$ μm filter, and a $10.8 \pm 0.19$ μm filter, this paper studies the relationship between the temperature and emissivity of graphite from 150 °C to 500 °C and calculates the relative error of temperature measurement respectively. A suitable fitting model which fits emissivity curves is selected. The measurement results show the use of a 10.2 μm filter to measure the graphite surface temperature has the smallest relative error, the range is 0.90%~1.17%. The emissivity of graphite with different roughness is also studied. At the same temperature, the greater the roughness of the graphite surface, the higher the emissivity value. The uncertainty of the emissivity measurement is analyzed, and its value is 0.0099–0.0211. The graphite surface temperature measurement method based on the emissivity model proposed in this paper provides useful references for the non-contact temperature measurement of the first wall in nuclear fusion devices. The research results can be used as a reference for plasma experiments in some fusion devices and other similar applications.

## 1. Introduction

Controlled nuclear fusion is currently one of the focus areas of science and technology. The research and development of controlled nuclear fusion technology may free humans from dependence on fossil energy in the future and completely solve the problem of energy shortage. Tokamak and stellarator are two main types of nuclear fusion devices which are containers using magnetic confinement to achieve controlled nuclear fusion. During the operation of the device, plasma continuously interacts on the first wall. Prolonged interaction between plasma and plasma-facing components deteriorates the wall material. Eventually, a higher thermal load is formed on the first wall [1]. Therefore, it is necessary to monitor the temperature of the first wall while operating the device, which is an important prerequisite for ensuring the safe and stable operation of the device.

Since the first wall material must have the characteristics of high melting point, thermal shock resistance, low outgassing rate, low corrosion, non-magnetic. After a lot of research, it is found that graphite fully meets these requirements. Graphite is a solid element widely found in nature with the advantages of high-temperature resistance, low thermal expansion coefficient, electrical and thermal conductivity, and thermal shock resistance. Thus, it is an ideal material used as a high-temperature resistant plasma-facing component material [2]. To better understand the temperature characteristics of graphite, it is necessary to study the emissivity characteristics firstly.

Traditional contact temperature measurement methods, such as

* Corresponding author.
*E-mail address:* zhangyuzhong@hfut.edu.cn (Y. Zhang).

https://doi.org/10.1016/j.nme.2022.101182
Received 8 November 2021; Received in revised form 31 March 2022; Accepted 8 April 2022
Available online 10 April 2022

using thermocouples to measure temperature, can accurately measure the temperature of the target. However, using thermocouples to measure temperature in nuclear fusion devices still has disadvantages. First of all, the thermocouples need a certain response time and the temperature indication lags behind the true temperature increase during the rapid heating process. Secondly, the distribution of thermocouples is limited. It cannot display a wide range of continuous temperature field distribution. During the operation of the device, it is necessary to provide timely diagnostic data and a continuous evaluation of the temperature field. The traditional thermocouple temperature measurement method is difficult to meet the needs of practical applications. Therefore, infrared cameras with high resolution and non-contact temperature measurements are widely used in the nuclear fusion devices, such as W7-X, JET, MAST, EAST, and other devices [3–5]. The infrared thermography system technically measured a photon flux, from which the surface temperature can be calculated, given an assumption about the emissivity. In this study, the measured infrared temperature refers to this inferred value. For example, the visible-infrared integrated system is used in the EAST infrared temperature measurement system, but the use of the infrared camera to measure temperature in a non-contact method will be affected by the surface effect of the measured object and the emissivity of the material. The strong plasma-material interaction changes the surface of the object, leading to incorrect estimation of the surface temperature [6]. Surface layers can change the emissivity of the surface, which is not addressed in this study. In the MAST device, the carbon wall is susceptible to surface effects and emissivity, which leads to errors when the infrared camera measures the temperature of fine-grained graphite on MAST-U. M. J. Dunn, T. W. Morgan, and other researchers measured the temperature with a medium-wave infrared camera and found the temperature of the carbon wall exposed to the plasma dropped by about 70 °C in 3 h [7]. As we know, the emissivity of a material is affected by many factors such as the object material, temperature, surface roughness, etc. [8]. At present, many devices use a combination of blackbody furnace calibration and high-temperature furnace temperature measurement to study the relationship between emissivity and temperature. There are also some methods dedicated to the development of emissivity models to measure temperature. The International Thermonuclear Experimental Reactor (ITER) will also employ an infrared camera system to study the relationship between the emissivity of the target plate and the temperature of the target plate and the life cycle of the target plate [9,10]. It can be seen that improving the temperature measurement accuracy of infrared thermal thermography is important to the research on emissivity.

In addition to real-time monitoring of the temperature of the first wall material in the device, there are also many experiments using infrared cameras to measure temperature and emissivity [11–13]. D. Ren et al. proposed a spectral emissivity measurement method based on two-sample heating methods of plate furnace and tube furnace to study the influence of temperature on the emissivity of graphite [14]. X. Song et al. used the integrated blackbody method to measure the infrared spectral emissivity of graphite at 1000–1500 °C [15]. They proposed a measurement method based on the optimization of the radiation method and the contact method, which effectively avoided the problem of measuring the true temperature of the material surface. Y. Zhang et al. studied the effects of temperature, surface roughness, and heating time on the emissivity of tungsten, graphite, and molybdenum in the wavelength range of 7.5–13 μm, and used different functional models to fit the relationship between the emissivity and temperature [16]. S. Alaruri et al. studied the use of a 1.6 μm single-wavelength pyrometer to measure the spectral emissivity of alloys and yttria-stabilized zirconia (YSZ) thermal barrier coatings at high temperature, providing an idea for the next single-wavelength measurement of emissivity [17]. C. Meola et al. used the Long-Wavelength Infrared and the Quantum Well Infrared Photodetector (QWIP) thermography to measure the small temperature change [18]. J. Gaspar et al. used an infrared camera to study the emissivity of tungsten-coated graphite in the WEST Tokamak divertor based on double heating and analyzed the distribution of emissivity [19], providing a useful reference for future study.

Due to the uncertainty of the emissivity of the graphite surface and the influence of related factors, the accuracy of the first wall temperature measurement by the infrared camera in the special applications of the nuclear fusion device, that is, under the vacuum and high-temperature environment, needs to be further improved. Considering the particularity of nuclear fusion devices, the engineering of its testing and temperature adjustment is huge and difficult to realize. Based on the current operating environment of the device and the infrared temperature measurement technology widely used in the temperature diagnosis system, this work designs and builds an emissivity measurement equipment based on infrared thermography to measure the surface temperature of graphite under experimental conditions as same as nuclear fusion devices. Focusing on the measurement method for graphite to improve the accuracy of temperature, this paper proposes a method to measure the surface temperature of graphite using an infrared camera with different wavelength filters and without the filter. The accuracy of graphite surface temperature measurement is improved by using a single wave filter. The uncertainty of the graphite emissivity measurement results is discussed. Different curve fitting formulas are compared to obtain the appropriate curve fitting equation, and the influence of different roughness on the graphite emissivity-temperature characteristics are analyzed. This paper will provide useful references for the non-contact temperature measurement of the first wall of nuclear fusion devices. The rest of this paper is organized as follows: The experimental setup and principle of graphite surface emissivity measurement using an infrared camera are described in detail in Section II. The experimental results of device calibration, uncertainty quantification, and graphite emissivity measurement are presented in Section III. Conclusions are given in Section IV.

## 2. Experimental setup and experimental methods

### 2.1. Experimental setup

This experiment is mimicking the environment in a nuclear fusion device. The temperature measurement device consists of a high-temperature furnace, a temperature controller, infrared camera, a water cooling device, a vacuum pump, and filters with different wavelengths. The schematic diagram of the temperature measurement device is shown in Fig. 1 and the experimental setup is shown in Fig. 2. The furnace is held in place externally by four stainless steel locking rings, with the ZnSe window in the middle. The furnace door is surrounded by water pipes to reduce the temperature of the door through water circulation. The furnace chamber of the high-temperature furnace is made of alumina with a size of 100 mm × 100 mm × 200 mm. Graphite is placed in the furnace chamber, and the graphite is fixed by a fixture. The surface temperature of the graphite is directly measured by close contact with the thermocouple installed on the inner wall of the high-temperature furnace. The thermocouples are S-type platinum-rhodium thermocouples to realize temperature measurement for the rear surface of the sample by spot welding, and the temperature controlling error is within 2 °C. The FLIR A40M is employed in this work with the band wavelength range of 7.5–13 μm. The recommended measurement range is (−40:500) °C, with a detector resolution of 240 × 320 pixels. The water cooling device is mainly used to control the temperature of the high-temperature furnace and reduce the background radiation. The vacuum pump is used to adjust the air pressure in the high-temperature furnace so that the furnace is kept close to the vacuum state. The vacuum pump keeps the pressure at constant 0.8 Pa during the experiment, including the slow heating ramp. The data processing system is connected to the infrared camera, which can collect data from thermal images. Three thermal images are collected during one temperature ramp and each thermal image is acquired every thirty seconds. The experiment is constructed to investigate whether the filter can improve

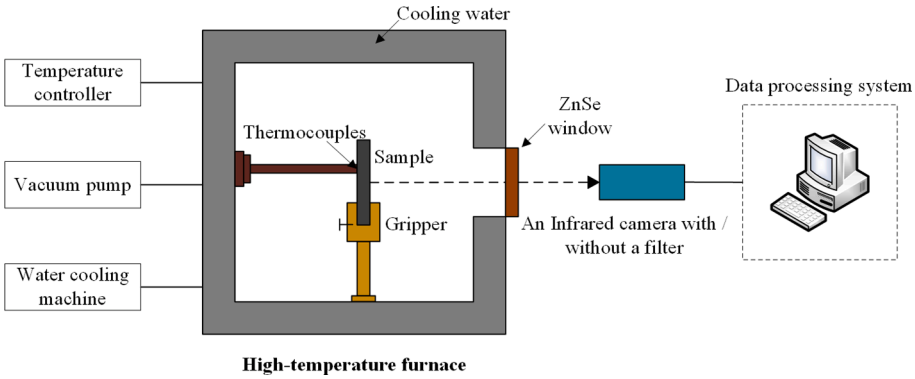


**Fig. 1.** The schematic diagram of the temperature measurement device.

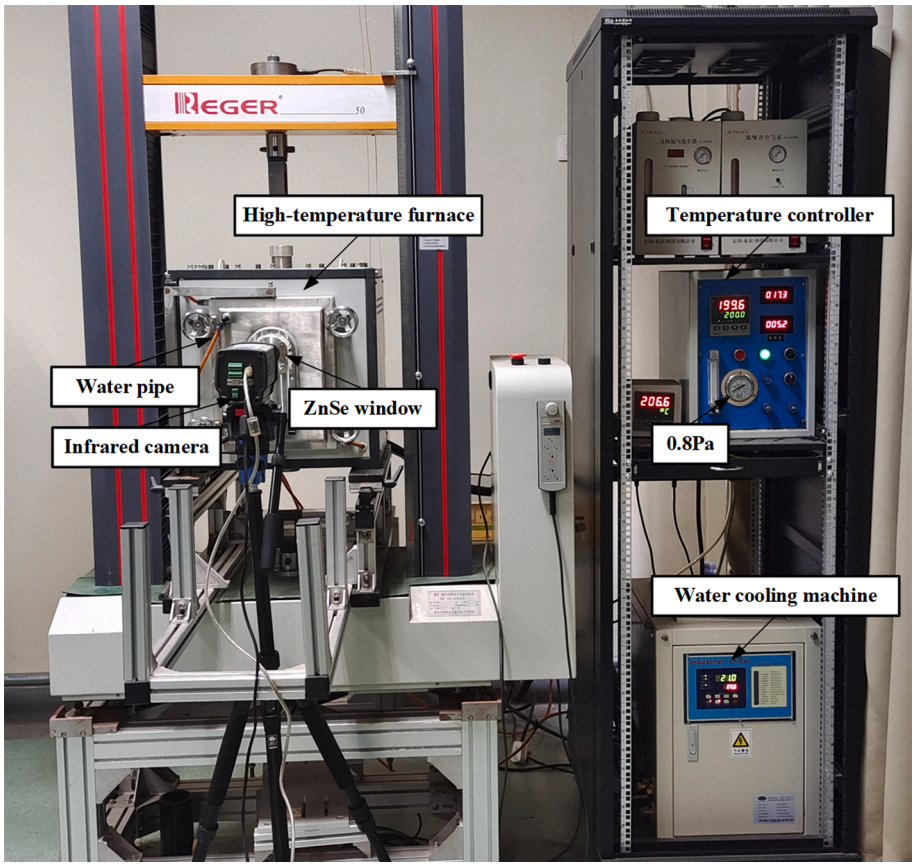


**Fig. 2.** Experimental setup.

the accuracy of measuring the temperature of the graphite surface. Besides the mostly transparent ZnSe window, two filters of 10.2 ± 0.1 μm and 10.8 ± 0.19 μm are used in the experiment and installed in front of the lens of the infrared camera. The experiment is carried out in three conditions: no filter (band wavelength range of 7.5 μm–13 μm), 10.2 μm filter, and 10.8 μm filter. The relationship between emissivity and temperature at different wavelengths is studied and the temperature measurement accuracy under three conditions is compared. In the experiment, the surface of the sample in the high-temperature furnace is perpendicular to the light path received by the infrared camera. As a result, we conduct the study on the normal emissivity of the sample. In the following content of the manuscript, all the "emissivity" represent the normal emissivity.

Before using the high-temperature furnace and the infrared camera for temperature measurement, the experimental device needs to be calibrated. The purpose of calibration is to obtain the value of the unknown parameters in Eq. (7) (detailed description in the following subsection 2.2). Therefore, the blackbody furnace is used for calibration. The calibration device consists of a blackbody furnace, a temperature controller, an infrared camera, and filters of different wavelengths. The schematic diagram of the calibration device is shown in Fig. 3. The blackbody furnace adopts the type 878 spherical high-temperature blackbody radiation source of Isothermal Technology Limited in the UK. Its heating temperature range is 100–1300 °C, and the temperature set in the calibration process of the experiment is 100–500 °C. Its emissivity is better than 0.999 and is considered as a black body.

### 2.2. Experimental principles and methods

The graphite is heated to a temperature of $T_{obj}$ in the high-temperature furnace. The infrared camera is placed in front of the high-temperature furnace, and a single wave filter is placed in front of

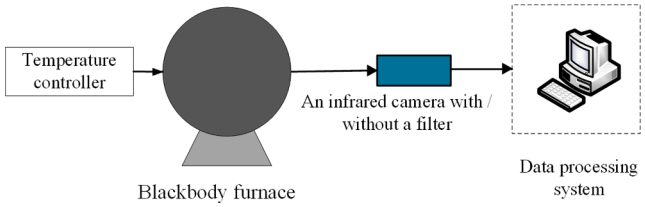


**Fig. 3.** The schematic diagram of the calibration device.

the lens of the infrared camera. At this time, the temperature of graphite measured by the infrared camera is $T$, and the radiation intensity from graphite received by the infrared camera is $E(\lambda_0, T)$, which can be expressed as Eq. (1):

$$E(\lambda_0, T) = C(\lambda_0) \times S \times P \times \delta \times E_{furnace} + E_0(\lambda_0) \tag{1}$$

where $C(\lambda_0)$ is the instrument response coefficient when the infrared camera incident wavelength is $\lambda_0$, $S$ is the detected target area, $P$ is the average transmittance of ZnSe window, $\delta$ is the average transmittance of filter, and $E_0(\lambda_0)$ refers to the radiation emitted by the infrared camera itself at wavelength $\lambda_0$. These parameters need to be calibrated by the black body furnace to obtain the determined values. $E_{furnace}$ refers to the intensity of radiation emitted in the furnace, Eq. (1) can be changed to Eq. (2):

$$E_{furnace}(\lambda_0, T) = [E(\lambda_0, T) - E_0(\lambda_0)]/[C(\lambda_0) \times S \times P \times \delta] \tag{2}$$

The radiation intensity emitted from the high-temperature furnace is not only emitted from the graphite's surface. As a result, we analyze the radiation source of the radiation emitted from the high-temperature furnace. It is learned that $E_{furnace}$ consists of the radiation of the following three parts:

(a) Radiation emitted from the surface of graphite, radiation intensity is $E_{surface}$:

$$E_{surface}(\lambda_0, T_{obj}) = \varepsilon \times E(\lambda_0, T_{obj}) \tag{3}$$

where $\varepsilon$ is the emissivity of the graphite surface, $E(\lambda_0, T_{obj})$ is the radiation intensity of the black body at the same temperature as graphite and wavelength $\lambda_0$.

(b) Radiation emitted from the inner wall of the high-temperature furnace is reflected from the graphite surface with the intensity of $E_{refl}$:

$$E_{refl}(\lambda_0, T_1) = \varepsilon_1 \times E(\lambda_0, T_1) \times (1 - \varepsilon) \tag{4}$$

where $\varepsilon_1$ is the emissivity of the inner wall of the high-temperature furnace. The emissivity of the inner wall of the high-temperature furnace is approximately regarded as the emissivity of the black body, so $\varepsilon_1 \approx 1$. $E(\lambda_0, T_1)$ is the radiation intensity of the blackbody when the wavelength is $\lambda_0$ and the temperature is the same in the high-temperature furnace, $T_1$ is the temperature in the high-temperature furnace. The temperature of the furnace is rising until the heating temperature arrives at 500 °C.

(c) Radiation emitted from the graphite surface is repeatedly reflected from the inner wall of the high-temperature furnace and the graphite surface, and the radiation intensity is $E_{again}$:

$$E_{again}(\lambda_0, T_1) = \varepsilon_1 \times E(\lambda_0, T_1) \times (1 - \varepsilon_1)^{m-1} \times (1 - \varepsilon)^m \tag{5}$$

where $m$ refers to m times of reflection. Since $\varepsilon_1 \approx 1$, the value of $E_{again}$ tends to be 0. Therefore, the radiation emitted from the high-temperature furnace:

$$E_{furnace}(\lambda_0, T_{obj}, T_1) = \varepsilon \times E(\lambda_0, T_{obj}) + (1 - \varepsilon) \times E(\lambda_0, T_1) \tag{6}$$

The emissivity expression can be obtained by substituting around Eqs. (2) and (6):

$$\varepsilon(\lambda_0, T, T_{obj}, T_1) = \frac{\frac{E(\lambda_0, T) - E_0(\lambda_0)}{C(\lambda_0) \times S \times P \times \delta} - E(\lambda_0, T_1)}{E(\lambda_0, T_{obj}) - E(\lambda_0, T_1)} \tag{7}$$

The calculation formula of radiation intensity E in Eq. (7) is shown in Eq. (8) [20]:

$$E(\lambda, T) = \int_{\lambda_2}^{\lambda_1} \frac{c_1 \times \lambda^{-5}}{\exp\left(\frac{c_2}{\lambda \times T}\right) - 1} d\lambda \tag{8}$$

where $c_1 = 3.7419 \times 10^{-16}$W·m$^2$ is the first radiation constant, $c_2 = 1.4388 \times 10^{-2}$m·K is the second radiation constant. $\lambda_1$ and $\lambda_2$ are the wavelength range of radiation received by the infrared camera. If no filter is added, the band wavelength range is from 7.5 to 13 μm, $\lambda_1 = 13$ μm, $\lambda_2 = 7.5$ μm. If one adds the wavelength filter (here with the wavelength of 10.2 μm and 10.8 μm) in front of the infrared camera, then it turns into a narrow band, $\lambda_1 = \lambda_0 + \Delta\lambda/2$, $\lambda_2 = \lambda_0 - \Delta\lambda/2$, and $\Delta\lambda$ is half of the wavelength width. When the wavelength is 10.2 μm, the value of $\Delta\lambda$ is 0.2 μm. When the wavelength is 10.8 μm, the value of $\Delta\lambda$ is 0.38 μm.

## 3. Emissivity measurement results and discussions

The emissivity measurement results of the graphite surface are divided into three parts, the first part is the result of the calibration by the blackbody furnace, the second part is uncertainty quantification and the third part is the results of the emissivity measurement of the graphite surface in the high-temperature furnace.

### 3.1. Calibration results

The calibration of the blackbody furnace is to obtain the unknown parameter values in Eq. (7). Firstly, the mean transmittance $P$ of the ZnSe window is calibrated. When no ZnSe window and a filter are installed, the radiation intensity $E(\lambda, T_{obj})$ emitted from the blackbody furnace and the radiation intensity $E(\lambda, T)$ measured by the infrared camera can be expressed by Eq. (9):

$$E(\lambda, T) = C(\lambda) \times S \times E(\lambda, T_{obj}) + E_0(\lambda) \tag{9}$$

In the calibration process of the blackbody furnace, eleven temperature points are set up, which are 100 °C, 140 °C, 180 °C, 220 °C, 260 °C, 300 °C, 340 °C, 380 °C, 420 °C, 460 °C, 500 °C. Fig. 4 shows the relationship between the radiation intensity emitted by the blackbody furnace and the radiation intensity measured by the infrared camera. As shown in Fig. 4, the value of $C(\lambda) \times S$ is 0.92762.

When the ZnSe window is added in front of the blackbody furnace, $E(\lambda, T_{obj})$ and $E(\lambda, T)$ can be expressed by Eq. (10):

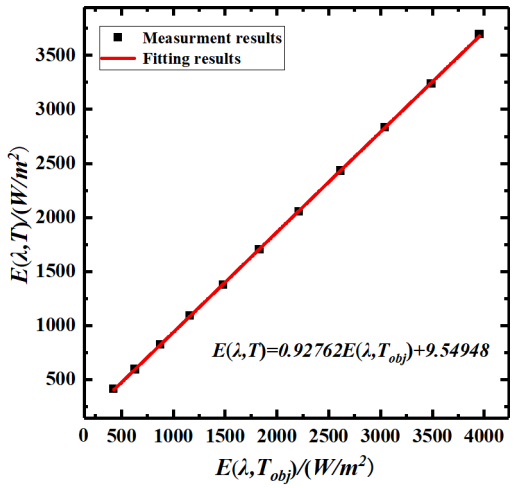


**Fig. 4.** Linear fitting without the ZnSe window and filter.

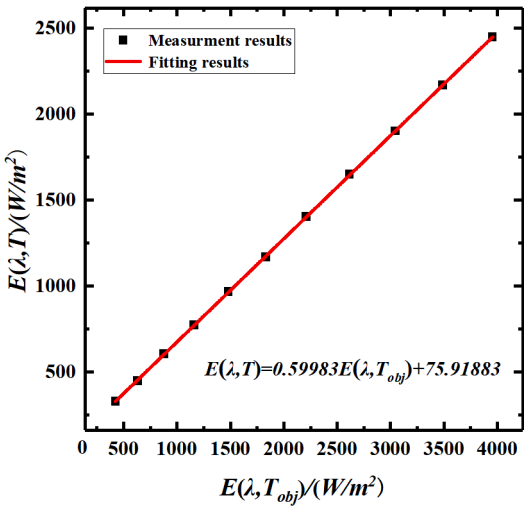


**Fig. 5.** Linear fitting with the Znse window.

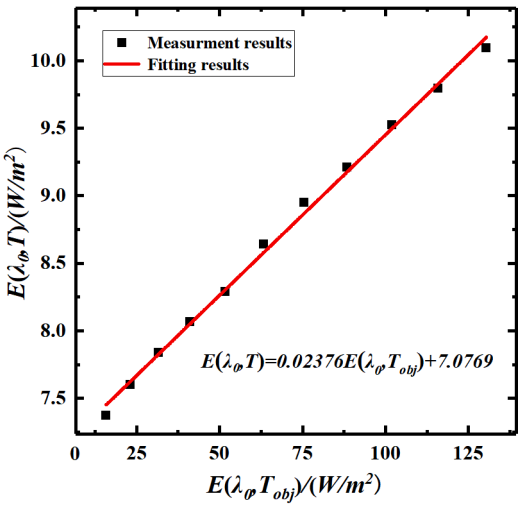


**Fig. 6.** Linear fitting with the ZnSe window and 10.2 μm filter.

$$E(\lambda, T) = C(\lambda) \times S \times P \times E(\lambda, T_{obj}) + E_0(\lambda) \tag{10}$$

Fig. 5 shows the relationship between the radiation intensity emitted by the blackbody furnace and the emission intensity measured by the infrared camera after the addition of the ZnSe window. As shown in Fig. 5, the value of $C(\lambda) \times S \times P$ is 0.59983, and the average transmittance $P$ of the ZnSe window is 64.66%.

In this experiment, for comparison, two wavelength filters of 10.2 μm and 10.8 μm are used respectively. So there are two calibration experiments. The 10.2 μm filter is added firstly. When a ZnSe window and filter are placed in front of the blackbody furnace, $E(\lambda_0,T_{obj})$ and $E(\lambda_0,T)$ can be expressed by Eq. (11):

$$E(\lambda_0, T) = C(\lambda_0) \times S \times P \times \delta \times E(\lambda, T_{obj}) + E_0(\lambda_0) \tag{11}$$

Fig. 6 shows the relationship between the radiation intensity emitted by the blackbody furnace with the ZnSe window and a 10.2 μm filter and the emission intensity measured by the infrared camera. As shown in Fig. 6, the value of $C(\lambda_0) \times S \times P \times \delta$ is 0.02376, the value of $E_0(\lambda_0)$ is 7.0769.

Finally, the 10.2 μm filter is replaced with the 10.8 μm filter. Fig. 7 shows the relationship between the radiation intensity emitted by the blackbody furnace and the emission intensity measured by the infrared camera after the addition of the ZnSe window and 10.8 μm filter. As shown in Fig. 7, the value of $C(\lambda_0) \times S \times P \times \delta$ is 0.02533, the value of $E_0(\lambda_0)$ is 12.9672.

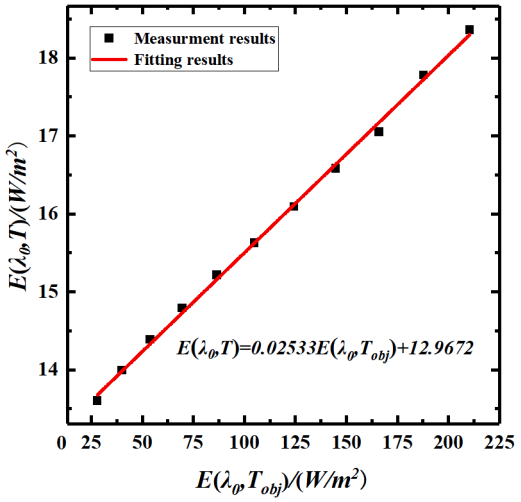


**Fig. 7.** Linear fitting with the ZnSe window and 10.8 μm filter.

### 3.2. Temperature and emissivity measurement results

#### 3.2.1. Uncertainty analysis

First of all, the sources of uncertainty of the measurement are analyzed. According to the principle of the measurement above described, the uncertainty can be divided into the following five parts: the first part is the radiation error $U_1$ caused by the infrared camera and graphite. The second part is the error $U_2$ generated when using the thermocouple to measure the graphite temperature. The third part is the temperature measurement error $U_3$ produced in the high-temperature furnace; The fourth part is the error $U_4$ caused by the radiation which is generated by the infrared camera. The fifth part is the error $U_5$ produced by the product of four parameters during the calibration by the blackbody furnace. The standard uncertainty components caused by these five factors are calculated respectively, and then the uncertainty of the measurement is obtained according to Eq. (12) [21]:

$$U_{eps} = \sqrt{\left(\left|\frac{\partial f}{\partial x_1}\right| U_1\right)^2 + \left(\left|\frac{\partial f}{\partial x_2}\right| U_2\right)^2 + \left(\left|\frac{\partial f}{\partial x_3}\right| U_3\right)^2 + \left(\left|\frac{\partial f}{\partial x_4}\right| U_4\right)^2 + \left(\left|\frac{\partial f}{\partial x_5}\right| U_5\right)^2} \tag{12}$$

The first three items belong to type B uncertainty, which are caused by experimental devices. They are approximately regarded as subject to a uniform distribution, which can be described by Eq. (13).

$$U_i = \frac{a}{\sqrt{3}} \quad (i = 1, 2, 3) \tag{13}$$

where $a$ is the value of the half-width of the distribution interval.

The latter two items in Eq.(12) belong to type A uncertainty, which is the uncertainty caused by repeated measurement three times, and the standard deviation of arithmetic mean value needs to be calculated. They can be described by Eq. (14).

$$U_i = \frac{\sigma_i}{\sqrt{n}} \quad (i = 4, 5) \tag{14}$$

where $n$ represents the number of repeated measurements, thus $n = 3$ in Eq. (14). $\sigma_i$ is the standard deviation of a single measurement.

Finally, the uncertainty of emissivity can be obtained by substituting Eq. (13) and Eq. (14) into Eq. (12). The uncertainty result of the measurement is shown in Fig. 8, and the uncertainty of the measuring device is 0.0099–0.0211 at different temperatures. The highest contributor is $U_4$ caused by the radiation which is generated by the infrared camera. During the experiment, there is a reflection between the filter and the infrared camera. As a result, it is a way to improve the reliability of the measurement by reducing the influence of reflections. The value of uncertainty is the largest at the temperature of 150 °C, which may be caused by the luminous flux. The luminous flux is relatively low in the case of lower temperatures, and the measurement has a certain degree of uncertainty. So in the picture of uncertainty analysis, when the temperature is 150 °C, the uncertainty is larger than the total spread of the emissivity values, not providing significant information to the fit.

### 3.2.2. *Influence of a filter on emissivity measurement accuracy*

For the three wavelength filters investigated, a piece of graphite is used to measure the emissivity and temperature in the experiment. Before each experiment, the dust in the chamber will be cleaned to avoid the reaction between dust and graphite. From the individual temperature ramps, data is acquired at the same steady state temperatures 150 °C, 200 °C, 250 °C, 300 °C, 350 °C, 400 °C, 450 °C, 500 °C. The sample surface temperatures are recorded and the images are read. However, the sample is clamped by the fixure, a small trace will be left below the graphite surface. The data of this part will not be used for the experimental result. According to Eq. (7), the emissivities of the sample at each temperature are calculated. The relationship between emissivity and temperature is obtained. To compare the influence of filters on the measurement accuracy of graphite surface temperature, it is necessary to calculate the relative error between the calculated value and the real value of graphite surface temperature without filter, with the filter of 10.2 μm and 10.8 μm respectively. Fig. 9 shows the relationship between temperature and emissivity.

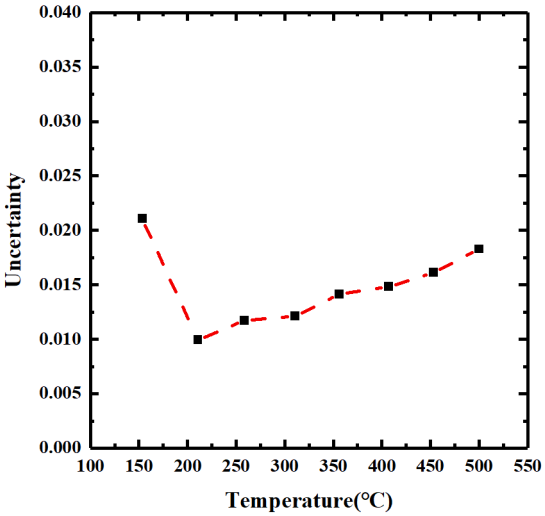


**Fig. 8.** Uncertainty analysis of absolute emissivity.

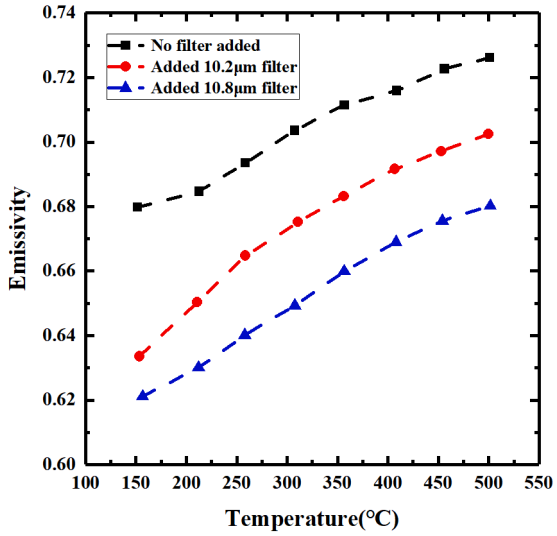


**Fig. 9.** The relationship between temperature and emissivity.

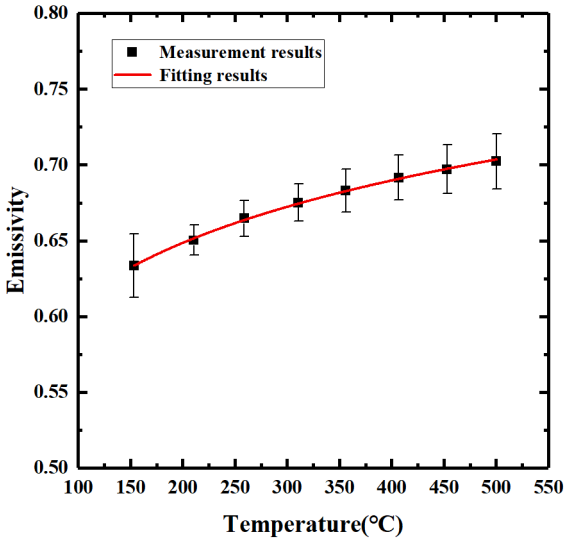


**Fig. 10.** The first curve fitting formula for temperature and emissivity.

**Table 1**
Parameters of the first curve fitting formula.

| | Value | Standard error | Dependency |
|---|---|---|---|
| *a* | 0.40555 | 0.00416 | 0.99686 |
| *b* | 0.08866 | 0.00179 | 0.99686 |

The real value of graphite surface temperature is obtained by the thermocouple. To compare the relative errors of temperature measurements in those three cases, it is necessary to get the calculated value of graphite surface temperature. Therefore, we need to estimate the parameters of the fitting formula which has been chosen before. During the curve fitting, two different curve fitting formulas are selected for comparison, and the curve with the smallest error is used to represent the relationship between emissivity and temperature. And the uncertainty analysis is applied to curve fitting.

The first curve fitting formula used in Fig. 10 is power-law, which is expressed by Eq. (15). The fitting result is shown in Fig. 10.

$$y = ax^b \tag{15}$$

The emissivity residuals of data and model at each temperature point are −0.00005, −0.00140, 0.00110, 0.00064, 0.00045, 0.00078, −0.00035, −0.00120. Mean value and standard deviation of emissivity residuals:

$$\overline{X}_1 = \frac{1}{n}\sum_{i=1}^{n} X_i = -0.000004 \tag{16}$$

$$S_1 = \sqrt{\frac{1}{n}\sum_{i=1}^{n}(X_i - \overline{X})^2} = 0.00085 \tag{17}$$

The second curve fitting formula is expressed by Eq. (18) [12]. The fitting result is shown in Fig. 11.

$$y = ax^{1/2} + bx + cx^{3/2} \tag{18}$$

The emissivity residuals of data and model at each temperature point are 0.00826, −0.00141, 0.00024, 0.00140, 0.00288, 0.00417, 0.00241, −0.00109. Mean value and standard deviation of emissivity residuals:

$$\overline{X}_2 = \frac{1}{n}\sum_{i=1}^{n} X_i = 0.00211 \tag{19}$$

$$S_2 = \sqrt{\frac{1}{n}\sum_{i=1}^{n}(X_i - \overline{X})^2} = 0.00294 \tag{20}$$

Compared with the mean value and standard deviation of emissivity residuals obtained by two fitting curves, the error of the first curve fitting formula is the smallest. So the first curve fitting formula is finally used to fit the relationship between temperature and emissivity. However, the dependency between the two parameters of the first fitting model is 0.99686 in Table 1, which represents a very strong correlation. This affects the reliability of optimization routines, and also the error analysis. As a result, it's necessary to modify the first fitting model (Table 2).

A solution is to re-parameterize the model. The correlation is caused by the term $T^b$ in Eq. (15), which scales the profile strongly, due to all T ≫ 1. This is compensated by using a reference temperature $T_{ref}$ to scale the basis of the power law:

$$y = \frac{a}{T_{ref}^b} \times T^b \tag{21}$$

Note that this corresponds to the more general approach of changing

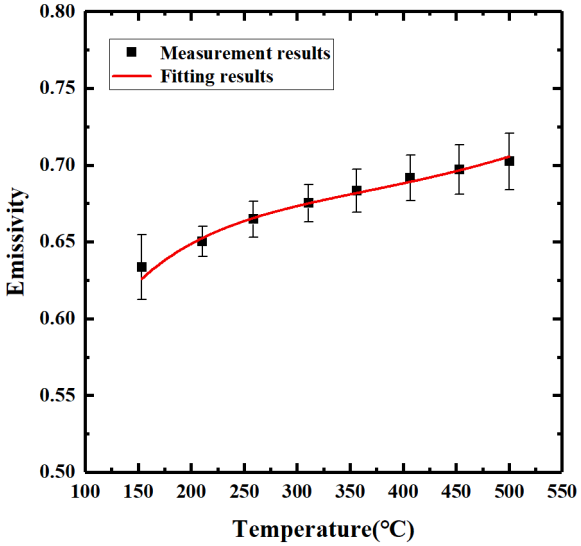


**Fig. 11.** The second curve fitting formula for temperature and emissivity.

**Table 2**
Parameters of the second curve fitting formula.

| | Value | Standard error | Dependency |
|---|---|---|---|
| *a* | 0.0994 | 0.00276 | 0.99949 |
| *b* | −0.00508 | 3.1055E-4 | 0.99988 |
| *c* | 9.13095E-5 | 8.57813E-6 | 0.99959 |

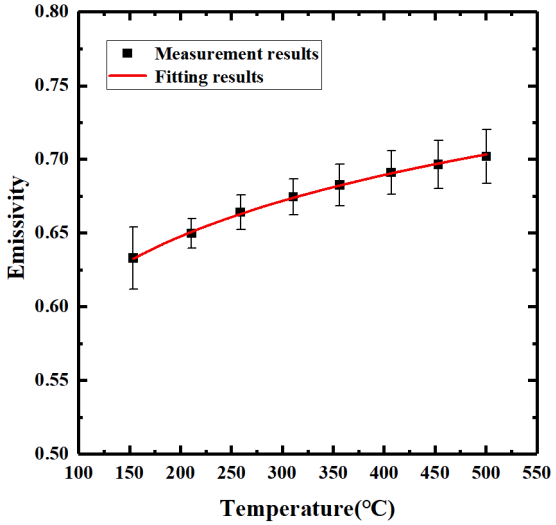


**Fig. 12.** Scaled power law.

**Table 3**
Parameters of scaled power law.

| | Value | Standard error | Dependency |
|---|---|---|---|
| *a* | 0.67728 | 3.89674E-4 | 0.05135 |
| *b* | 0.08965 | 0.00175 | 0.05135 |

the parameter *a* to:

$$a' = \frac{a}{\langle T \rangle^b} \tag{22}$$

therefore the name re-parameterization. Indeed the value of *a* and the correlation between the parameters change. The reference value is defined by the simple rule:

$$T_{ref} = \langle T \rangle = 325 \tag{23}$$

as the exact value is not strongly influencing the result, like the correlation of *a'* and *b*. The ideal value is problem dependent and not of interest for this analysis. The modified fitting curve is shown in Fig. 12 and the modified fitting curve is named as scaled power law.

According to Table 3, parameters of scaled power law are shown and it's found that the dependency between scale factor *a* and exponent *b* is 0.05135, which can be regarded as that scale factor *a* and exponent *b* are independent. The emissivity residuals of data and model at each temperature point are 0.00039, −0.00113, 0.00118, 0.00064, 0.00036,0.00059, −0.00061, −0.00151. Arithmetic mean and standard deviation of emissivity residuals:

$$\overline{X}_3 = \frac{1}{n}\sum_{i=1}^{n} X_i = -0.00001 \tag{24}$$

$$S_3 = \sqrt{\frac{1}{n}\sum_{i=1}^{n}(X_i - \overline{X})^2} = 0.00089 \tag{25}$$

In the process of temperature measurement, eight temperature

points including 150 °C, 200 °C, 250 °C, 300 °C, 350 °C, 400 °C, 450 °C and 500 °C are selected to draw the emissivity – temperature curve, and then the curve fitting formula with the minimum relative error is selected to carry out curve fitting. Next, it is necessary to use other temperature points to test the effect of the curve fitting formula selected, and observe whether it can maintain a good fitting effect at other temperature points. Therefore, six temperature points including 230 °C, 280 °C, 330 °C, 380 °C, 430 °C and 480 °C are selected to test the effect of curve fitting.

To test the effect of the modified fitting model, the residual of emissivity between experimental data and fitting model data and relative errors of emissivity is calculated. The residual of emissivity between experimental data and fitting model data are −0.00508, −0.00053, −0.00071, −0.00220, −0.00042, −0.00134. The relative errors of emissivity are 0.726%, 0.075%, 0.101%, 0.314%, 0.061%, 0.191%. Fig. 13 shows the emissivity-temperature diagram before and after using the scaled power law. It can be found that the residual between data and model is small. As a result, scaled power law can well describe the relationship between emissivity and temperature of graphite.

According to Eq. (6), the relative error between the real value and the calculated value is analyzed, and the mean value and mean square error of the relative error are used as evaluation indexes to judge the influence of the filter on the measurement accuracy of graphite surface temperature. Table 4 shows the relative error of each temperature point under the three conditions. Table 5 shows the arithmetic mean value and mean square error of relative error. It can be seen from the results that the mean value and standard deviation of relative error of temperature measurement with a 10.2 μm filter is the smallest (Table 6).

It can be concluded from Fig. 14 that adding a filter can improve the temperature measurement accuracy of the graphite surface, and the temperature measurement accuracy is the highest when a 10.2 μm filter is used.

### 3.2.3. *Influence of roughness on the emissivity of graphite*

After analyzing the influence of different wavelength filters on the measurement accuracy of graphite temperature, the influence of different roughness on the emissivity – temperature curve of graphite is studied. The emissivities of graphite with four different surface roughness are measured, and the emissivity – temperature curves of graphite with four different surface roughness are plotted.

It can be seen from Fig. 15 that at the same temperature point, the greater the surface roughness of graphite, the higher the emissivity of graphite. This is in line with earlier studies, for example in [22], but now

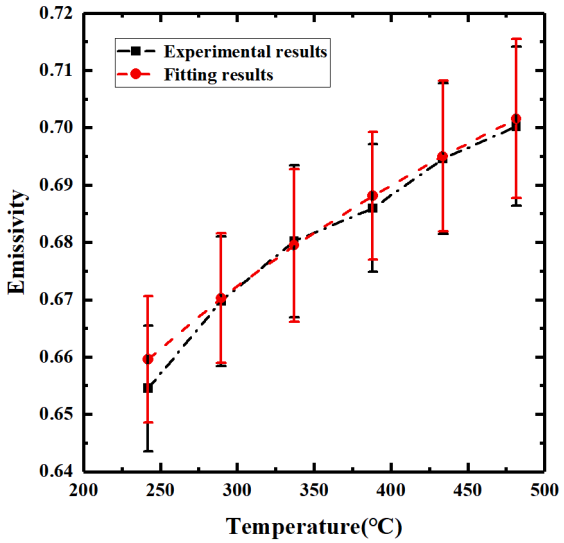


**Fig. 13.** Effect test of scaled power law.

**Table 4**
The relative error of each temperature point.

| Temperature (°C) | Without filter | 10.2 μm filter | 10.8 μm filter |
|---|---|---|---|
| 150 | 2.18% | 1.17% | 1.72% |
| 200 | 1.93% | 1.04% | 1.46% |
| 250 | 1.90% | 0.93% | 1.59% |
| 300 | 1.76% | 0.90% | 1.53% |
| 350 | 1.65% | 0.93% | 1.29% |
| 400 | 1.66% | 1.06% | 1.23% |
| 450 | 1.67% | 0.97% | 1.34% |
| 500 | 1.72% | 0.96% | 1.52% |

**Table 5**
The arithmetic mean value and mean square error of relative error.

| | Without filter | 10.2 μm filter | 10.8 μm filter |
|---|---|---|---|
| arithmetic mean | 1.80875 | 0.995 | 1.46 |
| Standard deviation | 0.1724 | 0.0838 | 0.1538 |

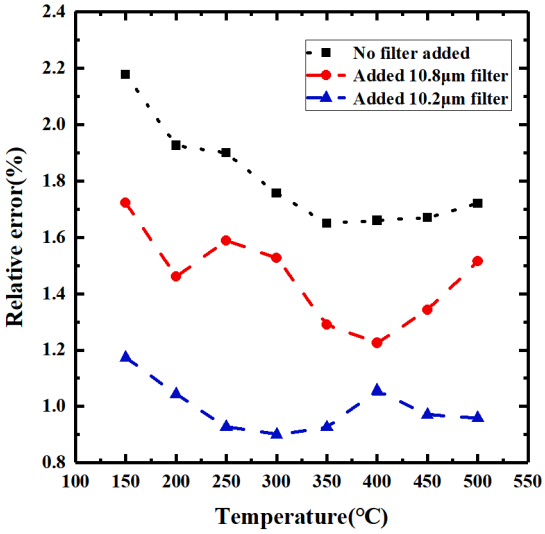


**Fig. 14.** The relative error in three cases.

**Table 6**
Parameters of graphite surface roughness.

| Graphite | Ra(μm) | Rz(μm) | Rmax(μm) |
|---|---|---|---|
| Sample 1 | 6.907 | 31.92 | 43.7 |
| Sample 2 | 5.915 | 29.395 | 35.343 |
| Sample 3 | 3.66 | 21.595 | 25.7625 |
| Sample 4 | 1.41 | 9.53 | 12.1 |

quantified for plasma experiment relevant surface roughness values and with typically available thermography equipment. The greater the roughness, the more serious the degree of uneven graphite surface, and the greater the probability of radiation emitted by the graphite surface being received by the infrared camera after multiple reflections.

Fig. 16 shows the fitting curves with different surface roughness by using scaled power law. Table 7 lists the parameter values of the four fitting curves.

The same fitting model is used to describe the relationship between emissivity and temperature when the surface roughness of graphite is different. To study the effect of the individual scale factor $a$, we set a single and shared value of exponent $b$. Then, we start to fit and express the relationship between scale factor $a$ and roughness. Fig. 17 shows the relationship between scale factor $a$ and roughness. The scale factor $a$

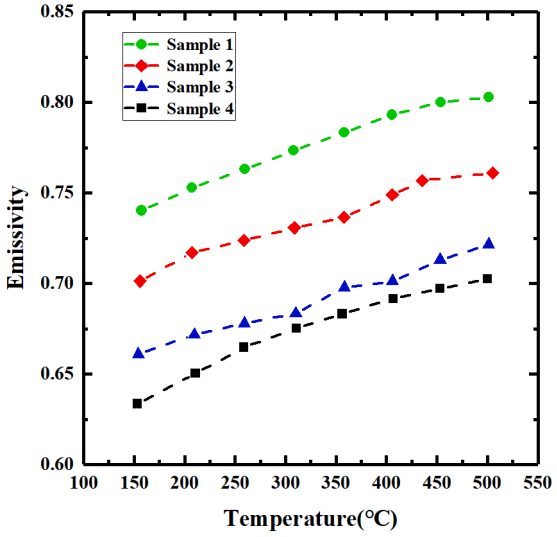


**Fig. 15.** Relationship between emissivity and temperature with different roughness of graphite.

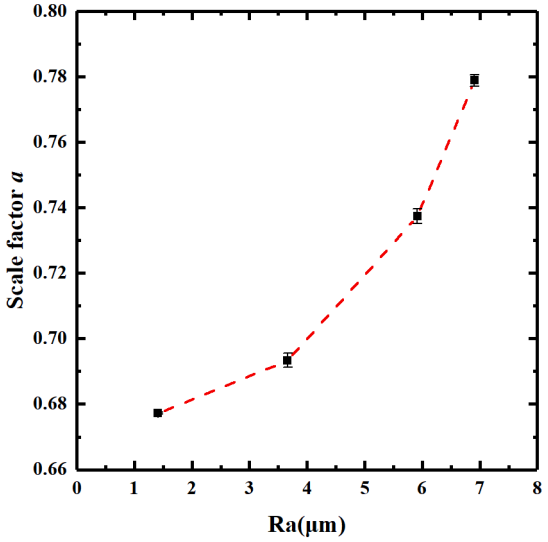


**Fig. 17.** The relationship between scale factor *a* and roughness.

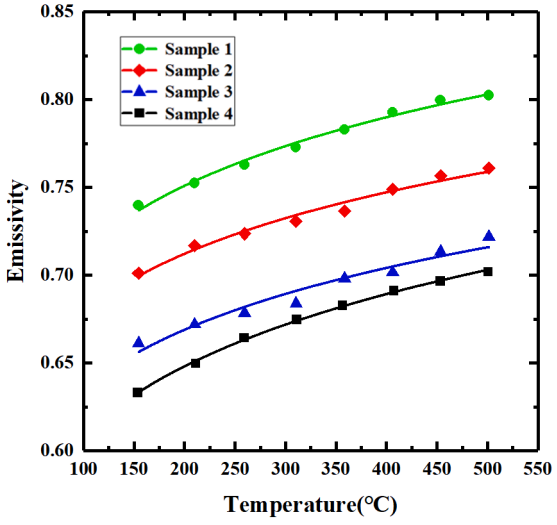


**Fig. 16.** Fitting curve by using scaled power law.

**Table 7**
Parameter values of the four fitting curves.

| | Sample 1 | Sample 2 | Sample 3 | Sample 4 |
|---|---|---|---|---|
| *a* | 0.77856 | 0.73667 | 0.6931 | 0.67724 |
| *b* | 0.07293 | 0.0691 | 0.07394 | 0.08855 |

increases as roughness increases in Fig. 17 because the value of emissivity is larger at the same temperature when the roughness is larger. If the value of exponent *b* is set as a fixed value, the roughness is larger, the emissivity is larger and the scale factor *a* is becoming larger.

## 4. Conclusions

Graphite is regarded as a material for the first wall of nuclear fusion devices. To accurately measure the temperature of the first wall, it is important to measure the surface emissivity of graphite. There are many methods to measure the surface temperature of graphite, such as contact measurement by thermocouples. However, to achieve accurate measurement in different working environments and conditions, non-contact measurement by using infrared cameras has been more and more widely used. In this work, the experiment is carried out using a FLIR infrared camera with no filter (band wavelength range of 7.5 μm–13 μm), a 10.2 ± 0.1 μm filter, and a 10.8 ± 0.19 μm filter respectively, and the emissivity of graphite is measured at 150 °C~500 °C in these three cases. At first, this paper studies the relationship between the temperature and emissivity of graphite and calculates the relative error of temperature measurement. The emissivity at given temperatures is systematically investigated. A suitable emissivity model which fits emissivity curves is finally selected. Comparing the results under three cases, it is concluded that using the filter can improve the measurement accuracy of the graphite surface and that the temperature measurement accuracy is the highest when a 10.2 μm filter is used. The experimental results show that in the range of 150–500 °C, the average relative error is 0.995% while using the 10.2 μm filter. The mean of relative error is the largest when no filter is added, which is 1.80875%. In the experiment, the emissivity of graphite with different roughness is measured with the 10.2 μm filter, and the emissivity-temperature curve of graphite with different roughness is obtained. By studying the effect of roughness on the emissivity of graphite, it is found that the larger the surface roughness of graphite, the higher the emissivity. The emissivity increases with increasing temperature, and the average change of emissivity is 1.94 × 10ˆ-4/K when the 10.2 μm filter is added. The emissivity-temperature curve of graphite is fitted by a modified fitting model which is named as scaled power law and this fitting model can well represent the relationship between the emissivity and temperature of graphite. The uncertainty of the measurement is analyzed, and its value is 0.0099–0.0211.

In a summary, this paper proposes a method of measuring graphite surface temperature based on infrared thermography and finds that the accuracy of measuring graphite surface temperature can be improved by using a filter. The measurement principle and method are described in detail in this paper. It provides a suitable method for the non-contact measurement of graphite surface temperature and also presents a useful reference for the temperature detection of the first wall in nuclear fusion devices. The research results can be used as a reference for nuclear fusion devices and other similar applications.

*CRediT authorship contribution statement*

**Shuangbao Shu:** Investigation, Methodology, Writing – original draft. **Tianqi Wu:** Formal analysis, Software, Investigation. **Ziyi Wang:** Investigation, Validation. **Yuzhong Zhang:** Validation, Supervision. **Ziqiang Yang:** Data curation, Visualization. **Huajun Liang:** Software.

## Declaration of Competing Interest

The authors declare that they have no known competing financial interests or personal relationships that could have appeared to influence the work reported in this paper.

## Acknowledgments

The authors are grateful to the team from the Institute of Plasma Physics, Chinese Academy of Sciences, for their valuable suggestions and discussions. This work was supported by the Fundamental Research Funds for the Central Universities (Grant No. JZ2019HGTB0082), the National Natural Science Foundation of China (Grant Nos. 51505120). The authors would like to thank all the experimental participants.

## References

[1] C. J. Lasnier, et al., Nucl. Fusion 38 (1998) 1255–1249. https://doi.org/10.1088/0029-5515/38/8/209.
[2] M. Oya, et al., Nucl. Mater. Energy 13 (2017) 58–62, https://doi.org/10.1016/j.nme.2017.07.006.
[3] P. Andrew, et al., J. Nucl. Mater. 363 (2007) 1006–1010, https://doi.org/10.1016/j.jnucmat.2007.01.285.
[4] G. De Temmerman, et al., Plasma Phys. Control. Fusion 52 (2010), 095005, https://doi.org/10.1088/0741-3335/52/9/095005.
[5] M. Jakubowski, et al., Rev. Sci. Instrum. 89 (2018) 10E116, https://doi.org/10.1063/1.5038634.
[6] X. Li, et al., Infrared Phys. Technol. 98 (2019) 1–6, https://doi.org/10.1016/j.infrared.2019.01.016.
[7] M.J. Dunn, et al., Nucl. Mater. Energy 25 (2020), 100832, https://doi.org/10.1016/j.nme.2020.100832.
[8] F. Zhang, et al., Infrared Phys. Technol. 73 (2015) 275–280, https://doi.org/10.1016/j.infrared.2015.10.001.
[9] M. Takeuchi, et al., Fusion Sci. Technol. 69 (2016) 655–665, https://doi.org/10.13182/fst15-191.
[10] R.A. Pitts, et al., Nucl. Mater. Energy 12 (2017) 60–74, https://doi.org/10.1016/j.nme.2017.03.005.
[11] S. Shu, et al., Infrared Phys. Technol. 116 (2021), 103801, https://doi.org/10.1016/j.infrared.2021.103801.
[12] Y. Zhang, et al., Rev. Sci. Instrum. 89 (2018) 10J126, https://doi.org/10.1063/1.5034233.
[13] C. Ruset, et al., Fusion Eng. Des. 114 (2017) 192–195, https://doi.org/10.1016/j.fusengdes.2016.12.015.
[14] D. Ren, et al., Int. J. Thermophys 37 (2016) 51, https://doi.org/10.1007/s10765-016-2058-9.
[15] X. Song, et al., J. Infrared Millim. Waves 40 (2021) 204–213, https://doi.org/10.11972/j.issn.1001-9014.2021.02.011.
[16] Y. Zhang, et al., Infrared Phys. Technol. 88 (2018) 74–80, https://doi.org/10.1016/j.infrared.2017.11.017.
[17] S. Alaruri, et al., Opt. Lasers Eng. 30 (1998) 77–91, https://doi.org/10.1016/s0143-8166(97)00108-5.
[18] C. Meola, et al., Infrared Phys. Technol. 72 (2015) 195–203, https://doi.org/10.1016/j.infrared.2015.08.004.
[19] J. Gaspar, et al., Nucl. Mater. Energy 25 (2020), 100851, https://doi.org/10.1016/j.nme.2020.100851.
[20] V.K. Bityukov, et al., Bull. Lebedev Phys. Inst. 45 (2018) 46–50, https://doi.org/10.3103/s1068335618020033.
[21] L. del Campo, et al., J. Appl. Phys. 107 (2010), 113510, https://doi.org/10.1063/1.3431541.
[22] K. Yu, et al., Opt. Rev. 24 (2017) 540–548, https://doi.org/10.1007/s10043-017-0345-8.